

Fig. 3 Liquid position as a function of time for the liquid channel, the vapor channel, and the connecting slot.

the liquid channel of

$$U_1 = \frac{1}{2\pi R_1 b} \int_0^b u 2\pi R_1 dy = \frac{1}{b} \int_0^b \frac{b^2}{2\mu_l} (a\rho_l) \left[\left(\frac{y}{b} \right)^2 - 2 \frac{y}{b} \right] dy = -\frac{b^2}{3\mu_l} (a\rho_l) \quad (22)$$

Substituting, as before, results in expressions for the length of the liquid film in the liquid and vapor channels of

$$h_1 = L + U_1 \tau = L - \frac{R_1^2}{3\mu_l} (a\rho_l) \tau \quad (23)$$

and

$$h_3 = L + U_3 \tau = L - \frac{R_3^2}{3\mu_l} (a\rho_l) \tau \quad (24)$$

respectively. Using Eqs. (14), (15), (19), (23), and (24) the location of the liquid vapor interface in the liquid channel, vapor channel, and connecting slot, along with the interface for the wall films in both the liquid and vapor channels can all be determined for a constant acceleration applied over some time interval.

Conclusion

Figure 3 illustrates the change of the liquid column lengths in the liquid and vapor channels H_1 and H_3 , respectively, along with the difference between the two all as a function of time, τ . As illustrated, when H_1 decreases, H_3 experiences a corresponding increase. This results in the accumulation of the liquid in the end of the heat pipe opposite the direction of acceleration. If a constant acceleration is maintained for a sufficient period of time, both H_1 and H_3 will approach a constant value. If Eqs. (11), (14), and (15) are evaluated as the time over which the acceleration is applied approaches infinity; i.e., $\tau \rightarrow \infty$, the following relationships result:

$$H_{1,0} = L - \frac{A_3}{2a(A_1 + A_2)} \left[2aL - \frac{4\sigma}{\rho_l} \left(\frac{1}{R_1} + \frac{1}{R_2} \right) \right] \quad (25)$$

$$H_{3,0} = L - \frac{A_3}{2a(A_1 + A_2)} \left[2aL - \frac{4\sigma}{\rho_l} \left(\frac{1}{R_1} + \frac{1}{R_2} \right) \right] - \frac{2\sigma}{\rho_l a} \left(\frac{1}{R_1} + \frac{1}{R_2} \right) \quad (26)$$

and

$$H_0 = \frac{2\sigma}{\rho_l a} \left(\frac{1}{R_1} + \frac{1}{R_2} \right) \quad (27)$$

Equations (25) and (26) illustrate that the final length of the liquid column in both the vapor and liquid channels depends not only upon the time and magnitude of the acceleration and properties of the working fluid, but also on the geometric parameters of the heat pipe.

Obviously, the distribution of the working fluid in an operating heat pipe during periods of acceleration is of critical importance in determining the operational limits and performance characteristics. For the case of longitudinal accelerations, one of two situations will occur: either the evaporator will be completely flooded (i.e., when the evaporator region of heat pipe is opposite the direction of acceleration) or the evaporator will dryout (i.e., when the evaporator end is toward the acceleration). For the latter case, dryout of the circumferential wall grooves may result in a need for significant reductions in evaporator heat fluxes to permit rewetting of the circumferential grooves.

References

- ¹Alario, J., Haslett, R., and Kossan, R., "The Monogroove High Performance Heat Pipe," AIAA Paper 81-1156, Palo Alto, CA, June 1981.
- ²Ambrose, J., and Holmes, S. R., 1991, "Development of the Graded Groove High Performance Heat Pipe," AIAA Paper 91-0366, Reno, NV, Jan. 1991.
- ³Peterson, G. P., and Marshall, P. F., 1984, "Experimental and Analytical Determination of Heat Pipe Priming in Micro-G," *Research and Development in Heat Pipe Technology*, Vol. 1, edited by K. Oshima, JaTec Publishing, Tokyo, Japan, pp. 434-439.
- ⁴Peterson, G. P., and Annamalai, N. K., "A Differential Approach to Heat Pipe Priming in Microgravity," *Chemical Engineering Communications*, Vol. 52, No. 1-3, 1987, pp. 151-167.

Combined Conjugated Heat Transfer from a Scattering Medium

M. Kassemi*

NASA Lewis Research Center,
Cleveland, Ohio 44135

and

B. T. F. Chung†

University of Akron, Akron, Ohio 44325

Introduction

IN this paper conjugated heat transfer from a convecting and radiating fluid in a reflecting rectangular channel is investigated. The model is representative of many high-temperature engineering problems commonly encountered in fur-

Received Feb. 1, 1991; revision received July 18, 1991; accepted for publication July 18, 1991. Copyright © 1991 by the American Institute of Aeronautics and Astronautics, Inc. All rights reserved.

*NASA/OAI Research Scientist, Processing Science and Technology Branch. Member AIAA.

†Professor, Department of Mechanical Engineering.

naces, boilers, combustion chambers, and nuclear reactors or nuclear rockets where the fuel elements consist of parallel heat generating plates cooled by a gaseous flow.

Previous investigations of combined heat transfer problems involving participating media are generally limited to constant temperature boundary conditions. Most of the recent investigators have included the effects of two-dimensional radiation. Among them, Kassemi and Chung¹ studied the simultaneous effect of scattering and wall reflection on convection in a rectangular channel; Smith et al.² performed a combined analysis including the spectral effects of gases; and Kim and Lee³ considered the effects of anisotropic scattering.

Unfortunately, none of the above investigations divulge any information about the effects of thermal radiation on the temperature distributions that develop in the walls. In many of the engineering applications mentioned above, the location and magnitude of the maximum wall temperature are important design and operational parameters. The wall temperature distributions are, in turn, controlled by the thermophysical properties of the system, the flow variables, and the radiative characteristics of the walls and the flowing medium. In many cases, the intervening fluid scatters thermal radiation. Scattering may be caused by the molecules of the fluid or by suspended solid particles or liquid droplets within the flow. The main thrust of this work is to indicate how scattering of radiation may affect the wall temperature distributions.

Formulation

Consider a hydrodynamically fully developed flow of a constant property fluid in a rectangular channel. The channel consists of two parallel heat conducting walls of finite length and height, and infinite width, as shown in Fig. 1. Heat transfer from the uniform heat generating medium is governed by conduction, convection, and two-dimensional radiation. The fluid is treated as an emitting, absorbing, isotropically scattering, gray medium. The walls of the channel are assumed to have diffuse gray inner surfaces and are of sufficiently small thickness so that wall conduction takes place only in the axial direction. These walls are subject either to an imposed external heat flux or equivalently to an internal uniform heat generation. The radiation environments at the inlet and outlet of the channel section are represented by two black sinks or pseudosurfaces. For a scattering medium, these environments are best approximated by pseudosurfaces with a net reflectivity equivalent to the overall reflectance of a semi-infinite isotropic medium. However, Stockham and Love⁴ have shown that, even for a highly scattering medium, the amount of back scattering from an infinite extent medium to its base is negligible and representation of these environments by black pseudosurfaces is adequate.

The inlet pseudosurface is held at the temperature of the inlet reservoir, which is also equal to the specified fluid temperature at the entrance. The outlet pseudosurface is assumed to be at a uniform temperature equal to the mixed mean temperature of the fluid at the exit. The energy equations governing combined heat transfer in the duct are as follows:

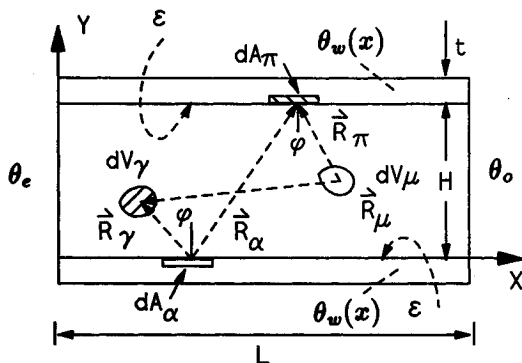


Fig. 1 The rectangular channel section.

$$(Ar \cdot Pe)u \frac{\partial \theta}{\partial x} = \frac{\partial^2 \theta}{\partial y^2} - \left(\frac{\tau_0}{N_g} \right) q + \frac{G_g}{N_g} \quad (1)$$

$$N_w \frac{d^2 \theta_w}{dx^2} + G_w = -N_g \frac{\partial \theta}{\partial y} \bigg|_w + q_w \quad \text{for } w = 1, 2 \quad (2)$$

where Ar is the aspect ratio; Pe is the Peclet number; τ_0 is the optical thickness; G_g and G_w are respectively the fluid and wall generation numbers; N_g and N_w are respectively the fluid and wall conduction-radiation parameters; u is the dimensionless Poiseuille velocity distribution; θ and θ_w are respectively the dimensionless temperatures of the fluid and the walls and q and q_w are respectively the dimensionless net radiative heat flux in the medium and at the walls.

Radiative heat transfer can be represented in terms of the following two equations:

$$\begin{aligned} & \left(\frac{1}{1 - \omega_0} \right) q - \left(\frac{\omega_0}{4(1 - \omega_0)} \right) \iiint_V q \left(\frac{1}{k_t} \frac{\partial^2 g_{\mu} g_{\gamma}}{\partial V \partial V_{\gamma}} \right) \\ & \cdot dV - \sum_{w=1}^2 \left(\frac{\rho_w}{1 - \rho_w} \right) \iint_{A_w} q_w \left(\frac{1}{k_t} \frac{\partial^2 w_{\alpha} g_{\gamma}}{\partial A \partial V_{\gamma}} \right) \\ & \cdot dA = 4\theta^4 - \iiint_V \theta^4 \left(\frac{1}{k_t} \frac{\partial^2 g_{\mu} g_{\gamma}}{\partial V \partial V_{\gamma}} \right) dV \\ & - \sum_{w=1}^2 \iint_{A_w} \theta_w^4 \left(\frac{1}{k_t} \frac{\partial^2 w_{\alpha} g_{\gamma}}{\partial A \partial V_{\gamma}} \right) dA - \iint_{A_e} \\ & \cdot \theta_e^4 \left(\frac{1}{k_t} \frac{\partial^2 s_{\alpha} g_{\gamma}}{\partial A \partial V_{\gamma}} \right) dA - \iint_{A_o} \theta_o^4 \left(\frac{1}{k_t} \frac{\partial^2 s_{\alpha} g_{\gamma}}{\partial A \partial V_{\gamma}} \right) dA \quad (3) \end{aligned}$$

$$\begin{aligned} & \left(\frac{1}{1 - \rho_w} \right) q_w - \left(\frac{\omega_0}{4(1 - \omega_0)} \right) \iiint_V q \left(\frac{\partial^2 g_{\mu} w_{\pi}}{\partial V \partial A_{\pi}} \right) \\ & \cdot dV - \left(\frac{\rho_w}{1 - \rho_w} \right) \iint_{A_w} q_w \left(\frac{\partial^2 w_{\alpha} w_{\pi}}{\partial A \partial A_{\pi}} \right) dA \\ & = \theta_w^4 - \iiint_V \theta^4 \left(\frac{\partial^2 g_{\mu} w_{\pi}}{\partial V \partial A_{\pi}} \right) dV - \iint_{A_w} \\ & \cdot \theta_w^4 \left(\frac{\partial^2 w_{\alpha} w_{\pi}}{\partial A \partial A_{\pi}} \right) dA - \iint_{A_e} \theta_e^4 \left(\frac{\partial^2 s_{\alpha} w_{\pi}}{\partial A \partial A_{\pi}} \right) dA \\ & - \iint_{A_o} \theta_o^4 \left(\frac{\partial^2 s_{\alpha} w_{\pi}}{\partial A \partial A_{\pi}} \right) dA \quad (4) \end{aligned}$$

Here, ω_0 is the scattering albedo; ρ_w and ϵ_w are respectively the surface reflectivity and emissivity, and k_t is the extinction coefficient; and θ_e and θ_o are respectively the temperatures of the inlet and outlet reservoirs. The quantities in the parentheses are the point to point exchange factors. For a detailed description of the formulation and the parameters, the reader is referred to Kassemi and Chung.¹

In view of the complexity of the problem, analytical solution of the governing equations is not feasible and numerical approach becomes inevitable. To generate numerical solutions, an element to node approach is adopted based on Hottel's zone method. Again, for details the reader is referred to Kassemi and Chung.¹ The accuracy of the computational scheme was checked through comparison with several limiting cases. In all the cases, agreement was found to be excellent with differences of less than 0.1%.

Results and Discussion

Because nine independent parameters are involved, presentation of a complete parametric study is not feasible. Only the cases where $\theta_e = 0.2$, $G_w = 1.0$; $G_g = 0$, are presented and the discussion is limited to show the effect of scattering and wall reflection on the conjugated heat transfer problem.

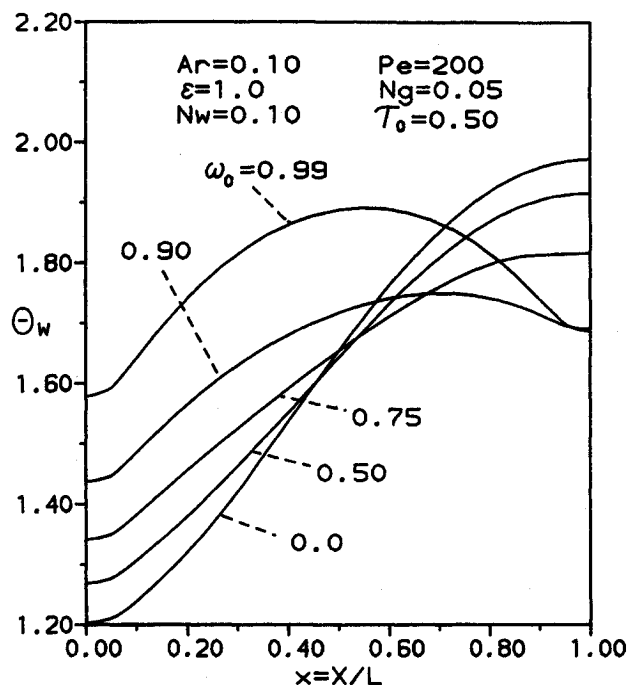


Fig. 2 Effect of scattering on the wall temperature distribution.

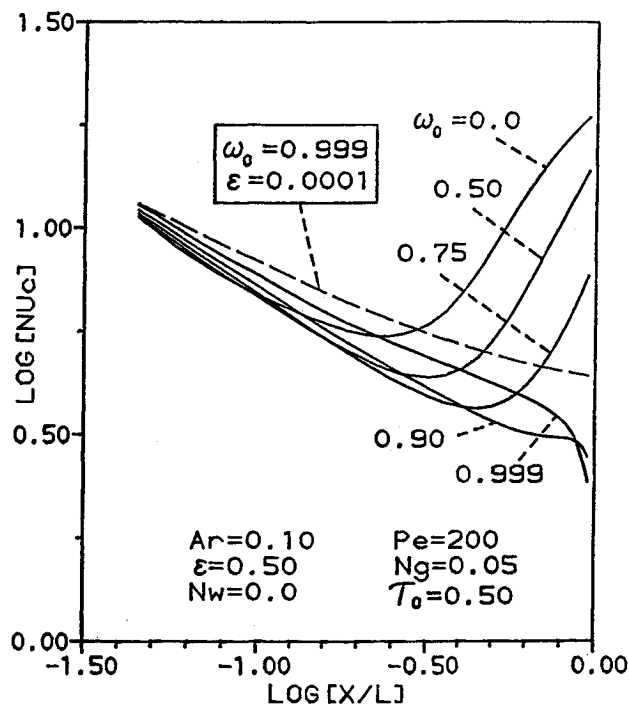


Fig. 3 Influence of scattering on the local convective Nusselt number.

Radiation scattering has a significant influence on the development of temperature profiles in the wall and in the medium. As evident in Figs. 2 and 3, it can affect the conjugated heat transfer process drastically. For low-to-moderate values of scattering albedo, the fluid actively participates in the radiative transfer process by absorbing the energy radiated from the hot walls, which is then redistributed by emission throughout the fluid and back to the walls. Our numerical results show that, because of this heat transfer augmentation effect of radiation, the mixed mean temperature of the medium rises very rapidly above the inlet value and levels off only near the end of the channel. The wall temperature profile shown in Fig. 2 follows a similar trend. Therefore, for example, for $\omega_0 = 0$, the maximum wall temperature occurs at the end of the channel. With an increase in scattering, the effects of radiation

are mitigated. As expected, for ω_0 above 0.90, there is almost no net radiation transfer in the fluid. The mixed mean temperature has a considerably smaller rise above its initial value at the inlet. Therefore, the temperatures of the inlet and outlet reservoirs are low compared to the wall temperature. Because of increased radiative loss to these end reservoirs, the temperature of the walls near the inlet and outlet decreases. Thus, in this situation, as shown in Fig. 2, the temperature distribution developed in the wall is parabolic and the maximum temperature shifts toward the middle of the channel.

Another interesting feature of this analysis is the behavior of the convective Nusselt number Nu_c . Fig. 3 illustrates the behavior of Nu_c (the constant heat flux case with $N_w = 0$) for the entire range of scattering albedos. It is evident that variation in scattering albedo has a great impact on Nu_c . At very high scattering albedos (ω_0 above 0.90), Nu_c decreases in the axial direction and drops sharply as the end of the channel is approached. This behavior is anticipated because increased radiative loss to the cold exit reservoir removes most of the heat imposed on the end region of the wall. Consequently, not as much heat must be removed by convection. It is interesting to note that in this case, when the net radiative loss from the wall is eliminated (by setting the surface emissivity equal to 0.0001), the sudden decline in Nu_c is no longer observed and an approach to a convective asymptotic value is evident. This is shown by the dashed curve in Fig. 3. The trend, however, changes significantly as participation of the medium in the radiative exchange is increased with a decrease in scattering; for example, $\omega_0 = 0.0$. At low scattering albedos, Nu_c decreases along the channel until a minimum value is reached beyond which it increases at a rapid rate. This behavior is explained by the state of thermal uniformity achieved by the medium where, because of the distributive nature of the emission-absorption process, the transverse temperature profile becomes almost flat and equal to the wall temperature. Therefore, again an approach to an asymptotic value is not observed.

Finally, our numerical results show that, although wall reflection has very little effect on the mixed mean temperature of the medium (fluid temperature in the core region is governed by convective and radiative transfer in the medium and is unaffected by wall radiation), it has a considerable effect on the wall temperature distribution. It is evident from Fig. 4 that as emissivity decreases, the wall temperatures increase

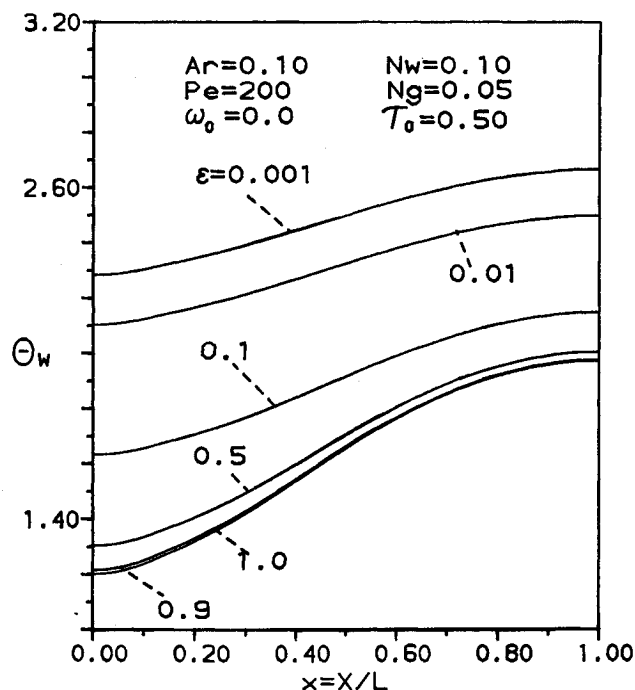


Fig. 4 Effect of wall emissivity on the wall temperature distributions.

and become more uniform. This is to be expected because the net radiative heat flux from the wall decreases as the wall surfaces become better reflectors and conduction becomes the dominant mode of heat transfer in the walls.

Conclusions

Combined heat transfer from a radiating and convecting flow of an absorbing, emitting, and scattering medium in a reflecting channel with conducting walls was numerically investigated. Our numerical results clearly indicate that in many high temperature applications, if the effects of scattering and wall reflection are ignored, the position and magnitude of the maximum wall temperature and the behavior of the convective Nusselt number can be grossly misrepresented.

References

- ¹Kassemi, M., and Chung, B. T. F., "Two-dimensional Convection and Radiation with Scattering From a Poiseuille Flow," *Journal of Thermophysics and Heat Transfer*, Vol. 4, No. 1, 1990, pp. 98–105.
- ²Smith, T. F., Byun, Ki-H., and Ford, M. J., "Heat Transfer for Flow of an Absorbing, Emitting and Isotropically Scattering Medium Through a Tube with Reflecting Walls," *Heat Transfer—Hemisphere Publ.*, Vol. 2, 1986, pp. 803–808.
- ³Kim, T., and Lee, H. S., "Two-Dimensional Convection and Radiation with Scattering from a Poiseuille Flow," *Journal of Thermophysics and Heat Transfer*, Vol. 4, No. 1, 1990, pp. 292–298.
- ⁴Stockham, L. W., and Love, T. J., "Radiative Heat Transfer from a Cylindrical Cloud of Particles," *AIAA Journal*, Vol. 6, No. 10, 1968, pp. 1935–1940.

Convective Heat Transfer of a Particulate Suspension

Ali J. Chamkha*

Fleetguard, Inc., Cookeville, Tennessee 38501

Introduction

HEAT transfer between a particulate suspension and a solid body is a problem whose solution involves the consideration of the equations of motion of a two-phase system. Both Soo¹ and Marble² have developed the conservation laws of mass, linear momentum, and energy for two-phase flow in general. These equations are sufficiently complex to preclude the possibility of exact solutions except in very idealized cases. Most closed-form solutions presently known are discussed by Soo¹ and Marble.²

The problem of steady single-phase flow of a Newtonian fluid past an infinite flat plate with uniform suction (the asymptotic suction profile) was given sometime ago by Schlichting.³ Chamkha and Peddieson⁴ reported exact solutions for the two-phase asymptotic suction profile. In their work, Chamkha and Peddieson⁴ did not consider the thermal aspects of the problem.

Received March 28, 1991; revision received Aug. 10, 1991; accepted for publication Aug. 21, 1991. Copyright © 1991 by the American Institute of Aeronautics and Astronautics, Inc. All rights reserved.

*Staff Research Engineer; also, Adjunct Assistant Professor, Mechanical Engineering, Tennessee Technological University, Cookeville, TN 38505. Member AIAA.

The purpose of this note is to report exact solutions for the temperature fields and the wall heat transfer for flow of a particle/fluid mixture past an infinite porous flat plate. The fluid phase is assumed to be incompressible and the volume fraction of suspended particles is assumed to be small. It is assumed, further, that the particles are sufficiently dilute and they do not interact with each other. It is also assumed that there is no radiative heat transfer from one particle to another. Numerical computations of the exact solutions are performed and a representative set of graphical results is presented and discussed.

Governing Equations

Consider the two-dimensional, steady, laminar, two-phase flow that takes place in a half-space bounded by an infinite porous flat plate. Let the flow be a uniform stream parallel to the x , y plane with the plate being coincident with the plane $y = 0$. Far from the plate, both phases are in equilibrium moving with a velocity V_∞ in the x direction. Uniform fluid-phase suction with velocity v_0 is imposed at the plate surface. Let the freestream suspension temperature be denoted by T_∞ and assume that the particle-phase density is constant. Because the plate is infinitely long, the fluid and particle velocity parallel to the plate, as well as the fluid and particle temperature, are independent of the x coordinate.

The dimensional form of the governing equations (which are based on the balance laws of mass, linear momentum, and energy for both the fluid and particulate phases) for the problem under consideration can be shown to reduce to

$$\begin{aligned} -\rho v_0 u' &= \mu u'' + \rho_p(u_p - u)/\tau_v \\ -\rho c v_0 T' &= k T'' + \mu(u')^2 + c_p \rho_p(T_p - T)/\tau_T \\ &+ \rho_p(u_p - u)^2/\tau_v \\ -\rho_p v_0 u_p' &= -\rho_p(u_p - u)/\tau_v \\ -\rho_p c_p v_0 T_p' &= -\rho_p c_p(T_p - T)/\tau_T \end{aligned} \quad (1)$$

where u is the fluid-phase velocity in the x direction, u_p is the particle-phase velocity in the x direction, T is the fluid-phase temperature, T_p is the particle-phase temperature, ρ is the fluid-phase density, ρ_p is the particle-phase density, μ is the fluid-phase dynamic viscosity, k is the fluid phase thermal conductivity, c is the fluid-phase specific heat at constant pressure, c_p is the particle-phase specific heat, τ_v is the velocity relaxation time (the time required by a particle to reduce its velocity relative to the fluid by e^{-1} of its original value in the unaccelerated state), τ_T is the temperature relaxation time (the time required for the temperature difference between a particle and fluid to be reduced to e^{-1} of its initial value), and a prime denotes ordinary differentiation with respect to y . It should be pointed out that the negative sign on the left-hand side of Eq. (1) is due to the fact that the suction velocity v_0 is in the direction opposite to the positive y direction and v_0 is the absolute value of the suction velocity. It can be seen from Eq. (1) that both phases are coupled through drag and heat transfer between them.

Substituting

$$\begin{aligned} y &= \nu\eta/V_\infty, & u &= V_\infty F(\eta), & u_p &= V_\infty F_p(\eta) \\ T &= T_\infty G(\eta), & T_p &= T_\infty G_p(\eta) \end{aligned} \quad (2)$$

(where ν is the fluid kinematic viscosity $\nu = \mu/\rho$) into Eq. (1) and rearranging yield

$$F'' + r_v F' + \kappa\alpha(F_p - F) = 0 \quad (3a)$$

$$\begin{aligned} G'' + r_v G' + \kappa P_r \gamma \epsilon (G_p - G) + E_c P_r (F')^2 \\ + E_c P_r \kappa\alpha (F_p - F)^2 = 0 \end{aligned} \quad (3b)$$